Local Dynamics of Polyisoprene in Toluene

Daniel J. Gisser, S. Glowinkowski,† and M. D. Ediger*

Department of Chemistry, University of Wisconsin, Madison, Wisconsin 53706

Received January 2, 1991; Revised Manuscript Received April 1, 1991

ABSTRACT: Local dynamics of polyisoprene in dilute solution with toluene are examined through ^{13}C NMR relaxation measurements. The variations of T_1 and NOE with Larmor frequency are analyzed over a wide temperature range, including both the extreme narrowing region and the T_1 minima. A frequency-temperature superposition of the data demonstrates that the distribution of motional time constants does not change shape with temperature and has a temperature and viscosity dependence consistent with that in nine other solvents. The data are analyzed in terms of eight motional models. Only those models that invoke motion on two well-separated time scales are successful. The slower, conformational motions correspond to activated torsional dynamics. The faster motions are librations within potential energy wells. Local dynamics in toluene are believed to exemplify polyisoprene dynamics in other solvents. Some similarities to local dynamics in bulk polymers are also expected.

I. Introduction

In recent years a great deal of effort has been devoted to understanding the local dynamics of polymers. This interest arises from the important role local polymer dynamics play in understanding structure-property relationships. In this paper we explore in detail the local dynamics of polyisoprene in dilute solution. This work is expected to be useful in two ways. First, a description of local dynamics may provide insight into dynamic mechanical behavior of polymer solutions. One specific example is the apparent modification of the high frequency limiting solvent viscosity in the presence of polymers.[1] Second, dilute polymer solutions provide a useful prototype for investigations of local dynamics in other environments. The effects of chain-chain interactions are minimized in dilute solution. As a result, attention can be focused on the internal motions of a single chain. Studies of dilute-solution dynamics should provide guidance in unraveling the more complex dynamics of bulk polymers.

This paper builds upon a previous study of local polymer motions.[2] In that work ^{13}C NMR relaxation measurements were employed to study local dynamics of polyisoprene in ten solvents. Here we examine in more detail the local dynamics of polyisoprene in one solvent, toluene. Polyisoprene solutions have previously been studied in our laboratories using time-resolved optical techniques[3-5] and Brownian dynamics computer simulations,[6] as well as NMR. Local dynamics of bulk polyisoprene have also been studied with ^{13}C NMR.[7-9]

^{13}C NMR relaxation measurements are sensitive to the reorientation of carbon-hydrogen bonds in the polymer chain. Quantitatively, the relaxation times depend upon the decay of the second-order orientation autocorrelation function

$$CF(t) = (1/2)\langle 3(\mathbf{e}_x(0)\cdot\mathbf{e}_x(t))^2 - 1\rangle \quad (1)$$

Here $\mathbf{e}_x(t)$ is a unit vector in the direction of the C-H bond at time t. The brackets indicate an ensemble average.

Our earlier work reports measurements from temperatures high enough that NMR relaxation times are in the extreme narrowing regime. At these temperatures all motions that contribute to $CF(t)$ are faster than the inverse of the Larmor frequency, and T_1s are independent of the Larmor frequency. When extreme narrowing conditions are satisfied, the mean relaxation time $\langle\sigma\rangle$ can be calculated directly from the spin-lattice relaxation time without reference to any motional model. In terms of the correlation function

$$\langle\sigma\rangle = \int_0^\infty CF(t)\,dt \quad (2)$$

In our previous work we[2] referred to $\langle\sigma\rangle$ as the correlation time, τ_c.[10]

The most important conclusion of our earlier work is that Kramers' theory[11,12] cannot describe the variation of $\langle\sigma\rangle$ with solvent viscosity. Kramers' theory predicts that $\langle\sigma\rangle$ increases linearly with η. In fact, the viscosity dependence is much weaker. Empirically, a power law relationship is found between $\langle\sigma\rangle$ and η in ten solvents. Thus

$$\langle\sigma\rangle = A\eta^\alpha e^{E_a/RT} \quad (3)$$

For polyisoprene $\alpha = 0.41 \pm 0.02$ and $E_a = 13 \pm 2$ kJ/mol. These values are properties of the polymer only. The constant $A \approx 0.3$ ps·cP$^{-\alpha}$, differing somewhat for chemically distinct C-H bonds. The fact that eq 3 is valid for ten different solvents implies that specific interactions between polyisoprene and the solvents do not determine the rate or mechanisms of local polymer motions. Futhermore, ratios of spin-lattice relaxation times for chemically different carbon nuclei, which are essentially determined by ratios of A for the different bonds, are independent of solvent and temperature.[2]

In this paper we ask, What types of motion are important in local dynamics? We will extract a more comprehensive picture of the local motions than could be obtained earlier. The conclusions discussed above indicate that the local dynamics of polyisoprene vary with temperature and viscosity but do not depend upon the solvent identity. Thus it is worthwhile to examine in more detail the dynamics in one solvent (toluene). We do this by considering the temperature dependence of T_1 relaxation data at multiple Larmor frequencies. We do not restrict attention to the extreme narrowing region. We also include the temperature range around the T_1 minima.

There are two equivalent ways to consider this problem. One point of view emphasizes the shape of $CF(t)$. Specific motional models provide predictions about the shape of $CF(t)$. These predictions can be tested with NMR or other experimental measurements or by computer simulations.[3,13,14] Alternately, one can consider a distribution of

* To whom correspondence should be addressed.
† On leave from the Institute of Physics, A. Mickiewicz University, Poznan, Poland.

0024-9297/91/2224-4270$02.50/0

motional time constants $F(\tau)$ which contribute to CF(t). The two points of view are related by a Laplace transform

$$\mathrm{CF}(t) = \int_0^\infty F(\tau)e^{-t/\tau}\,d\tau \tag{4}$$

We will emphasize the second approach here and ask what general features are required to fit the experimental relaxation time measurements. The major conclusion of this paper is that the distribution must be bimodal. Two distinct classes of motion, conformational and librational, are important in local dynamics.

II. Experimental Section

NMR measurements were made on 9.7 ± 0.2% (w/w) solutions of polyisoprene in toluene-d_8. Polyisoprene samples, obtained from two different sources, are characterized in Table I. Although the two samples had slightly different microstructures, the polymers displayed no significant differences in these experiments and were used interchangeably. Toluene-d_8 was purchased from Aldrich and Cambridge Isotope Laboratories. Solutions were passed through a 0.45-μm filter to remove very high molecular weight, cross-linked material. Dissolved oxygen was removed through several freeze–pump–thaw cycles. Samples were sealed under vacuum.

Spin–lattice relaxation times (T_1) and nuclear Overhauser enhancements (NOE) were measured under conditions of complete proton decoupling. Experiments were performed at ^{13}C Larmor frequencies of 125.8, 90.6, and 25.2 MHz using Bruker AM-500, AM-360, and AC-100 spectrometers, respectively. The data are plotted in Figures 3, 5, and 6. Much of the relaxation data collected at the two higher Larmor frequencies has been reported previously.[2] The sample temperature was controlled within 1 K. T_1 values are believed to be accurate within 10% and NOEs within 15%. Further details are provided in ref 2.

The labeling scheme used to identify the five carbon atoms in the polyisoprene repeat unit is

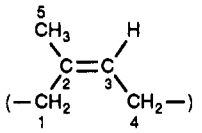

^{13}C NMR relaxation data from carbons C4 and C3 (δ = 26 and 125, respectively) in cis-1,4 linkages are analyzed in this paper.

Relaxation Equations. The dominant spin relaxation mechanism in these experiments is a dipole–dipole interaction between the backbone ^{13}C and its bonded proton(s).[2] Under these conditions T_1 and NOE may be expressed[15-18] in terms of the spectral density function $J(\omega)$

$$\frac{1}{T_1^{\mathrm{dd}}} = Kn[J(\omega_H-\omega_C) + 3J(\omega_C) + 6J(\omega_H+\omega_C)] \tag{5}$$

$$\mathrm{NOE} = 1 + \frac{\gamma_H}{\gamma_C}\left[\frac{6J(\omega_H+\omega_C) - J(\omega_H-\omega_C)}{J(\omega_H-\omega_C) + 3J(\omega_C) + 6J(\omega_H+\omega_C)}\right] \tag{6}$$

where γ_C and γ_H are the gyromagnetic ratios for carbon and hydrogen, ω_C and ω_H are their resonance frequencies, and n is the number of bonded protons. The constant K is given by

$$K = \frac{1}{10}\left(\frac{\mu_0\gamma_H\gamma_C\hbar}{4\pi}\left\langle\frac{1}{r^3}\right\rangle\right)^2 \tag{7}$$

where r is the C–H bond length. $J(\omega)$ is related to the correlation function

$$J(\omega) = \frac{1}{2}\int_{-\infty}^{+\infty}\mathrm{CF}(t)e^{i\omega t}\,dt \tag{8}$$

It is difficult to determine $\langle r^{-3}\rangle^2$, and thus K, precisely. We have assumed that the C–H bond length is harmonically constrained about its average r_0. The mean amplitude of vibration $\langle(r - r_0)^2\rangle^{1/2}$ is very nearly equal to 0.077 Å in many organic molecules.[19] We have used[20] r_0 = 1.09 Å for C4 and 1.08 Å for C3 and calculated $K = 2.29 \times 10^9$ s^{-2} for C4 and 2.42×10^9 s^{-2} for C3. Other authors have followed similar procedures.[21,22]

Table I
Polyisoprene Characterization

	source	
	Goodyear	Polysciences
M_w	10 200	10 200
M_w/M_n	1.11	1.11
% cis-1,4	76	68
% trans-1,4	18	27
% vinyl-3,4	6	5

Relaxation with nonbonded protons does not contribute significantly to the T_1s we report. Spin–lattice relaxation times of backbone carbon atoms are the same whether toluene-d_8 or toluene-h_8 is used as the solvent.[2] Thus, relaxation with solvent protons or deuterons is negligible. The efficiency of dipole–dipole relaxation diminishes with the sixth power of the distance separating the two nuclei. This allows an estimate that nonbonded protons on the same repeat unit and on neighboring repeat units of the same polymer chain account for 2% of the methylene and 7% of the methine carbon T_1s. On the basis of this estimate, relaxation with protons on the same chain that are far removed along the contour length but temporarily nearby in space is also likely to be negligible. The insensitivity of T_1s to solvent quality[2] supports this. Spin relaxation via dipole–dipole interaction with protons on neighboring polymer chains is also unimportant. T_1s are known to be independent of polymer concentration below about 15% polymer.[15] We have ignored all these small contributions from nonbonded protons to spin relaxation.

Chemical shift anisotropy accounts for 0–20% (depending on temperature and ω_C) of the spin relaxation for C3. Equation 5 can be modified to include this, leading to

$$\frac{1}{T_1} = \frac{1}{T_1^{\mathrm{dd}}} + \frac{1}{T_1^{\mathrm{CSA}}}. \tag{9}$$

where T_1^{dd} is the dipole–dipole contribution as in eq 5. If the chemical shift is axially symmetric, T_1^{CSA} is given by[17,18]

$$\frac{1}{T_1^{\mathrm{CSA}}} = \frac{2}{15}\omega_C^2(\sigma_\parallel - \sigma_\perp)^2 J(\omega_C) \tag{10}$$

Use of eq 10 is an approximation, as the electron distribution around C3 is not axially symmetric. Furthermore, the vector whose motion leads to CSA relaxation is not the C3–H bond but a vector determined by the electron distribution around C3. We have ignored these higher order effects and fit our data to eqs 5, 9, and 10 with[2] $(\sigma_\parallel - \sigma_\perp)$ = 150 ppm for C3 and $(\sigma_\parallel - \sigma_\perp) = 0$ for C4.

Fitting Procedure. Spin–lattice relaxation data were analyzed by using several trial spectral density functions (see section IV). We will show in section III that $F(\tau)$ does not change shape with temperature. The temperature dependence of $F(\tau)$ is given by

$$\tau_i = A[\eta(T)]^\alpha e^{E_a/RT} \tag{11}$$

where τ_i represents either τ_1 or $\bar{\tau}$, depending on the trial $J(\omega)$. All the other τ's in $F(\tau)$ are proportional to $\tau_i(T)$. We have fixed α = 0.41, as was determined from experiments in the extreme narrowing regime.[2] Values for E_a and A are also already known but have been treated as adjustable parameters in the fitting routine. This provides a check on the consistency of the fits. As E_a and A determine the temperature dependence of all τ in $F(\tau)$, we do not include τ_i when counting adjustable parameters. The viscosity $\eta(T)$ of toluene-d_8 is found in ref 2.

Temperature-dependent T_1s at all three Larmor frequencies were fit simultaneously. An iterative reconvolution routine utilized a nonlinear least-squares algorithm based on the Marquardt technique.[23] For the most complicated models of $F(\tau)$ five adjustable parameters were involved in the fitting procedure. Only the parameters A, E_a, and f were introduced into the fitting routine. All other parameters were varied "manually". Thus, the program never fit more than three parameters at once. An

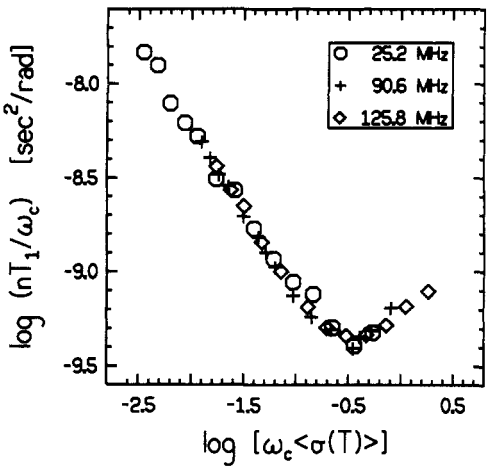

Figure 1. Frequency–temperature superposition of ^{13}C NMR spin–lattice relaxation times, nT_1, from the methylene carbon C4 of a 10% solution of polyisoprene in toluene-d_8. The raw data are plotted in Figures 3 and 4. The symbols correspond to different Larmor frequencies, $\omega_C/2\pi$. Experimental error bars (±10%) are given by the size of the symbols. This superposition demonstrates that the distribution of motional time constants has a shape that is independent of temperature.

instrumental uncertainty of 10% was assumed for each measurement. The best fit was judged to be that with the lowest χ_R^2.

III. Frequency–Temperature Superposition

The attempt to find an $F(\tau)$ consistent with temperature-dependent NMR relaxation data is greatly simplified if the mechanisms of local motions are known to be temperature independent. In such cases the shape of $F(\tau)$ is temperature independent. We have previously argued that this is true at high temperatures for polyisoprene in many solvents.[2] We now extend this conclusion to include the lower temperatures employed in this study.

Recently, Guillermo et al.[24] have demonstrated a method for superposing bulk polybutadiene T_1 data collected at different Larmor frequencies. This superposition is possible only if all the time constants that enter into an explicit expression for $F(\tau)$ have the temperature dependence of a characteristic time constant, $\tau_R(T)$. A plot of (ω_C/nT_1) versus log $[\omega_C\tau_R(T)]$ successfully superposes ^{13}C relaxation data from different Larmor frequencies. This indicates both that $F(\tau)$ has a shape independent of temperature and that the calculated temperature dependence is correct. The calculated variation of $\tau_R(T)$ with temperature is consistent with the WLF equation for polybutadiene.

We have applied a similar procedure to our T_1 relaxation measurements. For dilute solutions of polyisoprene, the temperature dependence of the local dynamics is given by eq 3 with A = 0.3 ps/cP$^\alpha$, α = 0.41, and E_a = 13 kJ/mol. This allows us to plot log (nT_1/ω_C) versus log $[\omega_C\langle\sigma(T)\rangle]$, analogous to the work of Guillermo et al. Figure 1 shows this plot for the methylene carbon C4 of polyisoprene in toluene-d_8. Data for the three Larmor frequencies superpose very well over the entire temperature range, even through the T_1 minima. This demonstrates that all of the motional time constants contributing to spin relaxation are proportional to $\langle\sigma(T)\rangle$ and justifies attempts to fit the data to temperature-independent distribution functions.

The methine carbon T_1 data can be plotted in the same manner as Figure 1. The C3 data do not superpose quite as well as those of C4, however. This is partially a reflection of the fact that chemical shift anisotropy (CSA) provides a competitive mechanism for C3 spin–lattice relaxation.[25] The CSA relaxation rate scales differently with ω_C than

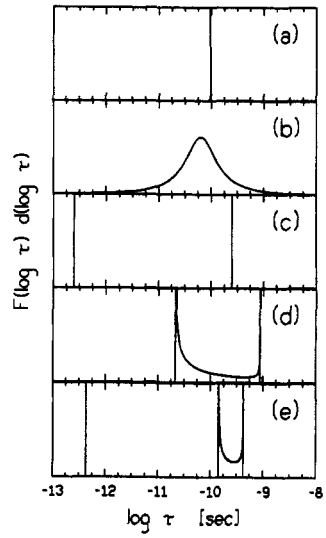

Figure 2. Distributions of motional time constants calculated for methylene carbon C4 at 250 K in toluene-d_8: (a) exponential correlation function; (b) Cole–Cole distribution, ϵ = 0.79; (c) biexponential, τ_1/τ_0 = 1000; (d) Hall–Helfand, τ_2/τ_1 = 20; (e) DLM, τ_2/τ_1 = 1, τ_1/τ_0 = 1000. All other parameters are as in Table II. The distributions shown in (c) and (e) provide adequate descriptions of the data; (a), (b), and (d) do not.

does the dominant dipole–dipole mechanism, as can be seen in eqs 5 and 10. Also, the C3 data are noisier than the C4 data, particularly near the T_1 minima.

The superposition shown in Figure 1 does not rigorously demonstrate that *all* the time constants τ involved in local dynamics have the temperature dependence of eq 3. Only motions with τ near $1/\omega_C$ provide major contributions to spin–lattice relaxation. Motions corresponding to time constants $\tau \ll 1/\omega_C$ can behave quite differently with temperature, yet not affect Figure 1 if the weighting of these very fast components of CF(t) does not change with temperature.

IV. Models

Many models of local polymer dynamics have been proposed.[16] Our goal is to discern the essential features necessary in a motional model. Less emphasis is given to finding the one model that best fits the data. We have fit the data to eight models. In each case the shape of $F(\tau)$ is taken to be temperature independent.

NMR is sensitive to $J(\omega)$, the Fourier transform of the correlation function, CF(t). T_1 becomes independent of ω_C only when $\tau \ll 1/\omega_C$ for all τ in $F(\tau)$. T_1 is short when ω_C is approximately equal to frequencies of local motion. Sharp distributions $F(\tau)$ predict deep and sharp T_1 minima. Broad distributions predict broad and raised minima. Mathematical forms for $F(\tau)$, $J(\omega)$, and CF(t) (where appropriate) are included for each model in the Appendix and references. Graphs of some best fit F(log τ) d(log τ) are presented in Figure 2. Salient features of each model are summarized here.

Single Exponential. The simplest description of local dynamics is an exponential CF(t), corresponding to a δ function around τ_1 in Laplace space (Figure 2a). This model has no free parameters (other than A and E_a, present for all models). At high temperature it predicts that T_1 is independent of ω_C (the extreme narrowing region).

Unimodal Distributions. Three unimodal distributions of motional time constants have been tested. Each distribution is centered about $\bar{\tau}$. The Cole–Cole distribution[15,26,27] provides a symmetric F(log τ) (Figure 2b). One parameter ϵ is introduced, with $0 < \epsilon \leq 1$. The Fuoss–

Table II
C4 T_1 Fit Parameters

model	width[a]	τ_1/τ_0	f	E_a, kJ/mol	A, ps/cP$^\alpha$	χ_R^2
exponential				10.1	0.70	5.9
Cole–Cole	0.79			14.3	0.062	4.3
Fuoss–Kirkwood	0.79			13.3	0.11	4.6
log χ^2	25			14.6	0.049	3.4
biexponential		10	0.60	12.1	0.70	3.4
		100	0.52	13.1	0.44	1.24
		1000	0.495	13.3	0.39	1.08
		10000	0.492	13.3	0.39	1.08
Hall–Helfand	20			13.4	0.066	3.5
DLM	1	1000	0.48	13.7	0.56	1.11
	5	1000	0.43	15.2	0.11	1.5
	10	1000	0.39	16.5	0.045	1.9
modified Cole–Cole	0.95	1000	0.47	14.5	0.20	0.99

[a] Width corresponds to ϵ, β, p, or τ_2/τ_1.

Kirkwood distribution[15,27,28] differs from the Cole–Cole distribution only in detail. The parameter ϵ is replaced by β, with $0 < \beta \leq 1$. The log χ^2 distribution[15,29] is asymmetric, skewed toward long τ's. The logarithm base b is conventionally chosen equal to 1000, and the width of the distribution is determined by a positive integer p. All three of these distributions recover the single-exponential CF(t) results when the appropriate parameter (ϵ, β, or p) takes on its maximum value.

Other Distributions. A biexponential CF(t) (Figure 2c) introduces two parameters, the ratio τ_1/τ_0 and f, the relative weight of the faster component, τ_0. Small ratios τ_1/τ_0 predict somewhat broadened T_1 minima relative to the single-exponential case. Large ratios and moderate values of f lead to high minima. If τ_1 and τ_0 are sufficiently well separated, two minima are predicted.

The Hall–Helfand[30,31] CF(t) has been used to describe local dynamics observed in time-resolved optical experiments[4,5] and Brownian dynamics simulations.[14] The corresponding spectrum of time constants (Figure 2d) diverges at $\tau = \tau_2$ and $\tau = (1/\tau_2 + 2/\tau_1)^{-1}$, with less density between these two critical values and no density outside of them. The only parameter introduced is the ratio τ_2/τ_1. Large values of τ_2/τ_1 provide a broad $F(\tau)$ and a high T_1 minimum, but unlike the unimodal distributions above, the Hall–Helfand $F(\tau)$ has sharp cutoffs at long and short τ. Therefore an attainable extreme narrowing region is predicted. Allowing $\tau_1 \to \infty$ recovers the single-exponential CF(t).

Dejean de la Batie et al.[8,31,32] have combined the Hall–Helfand and exponential functions, producing the DLM CF(t) (Figure 2e). This flexible function introduces three parameters, the ratios τ_2/τ_1 and τ_1/τ_0 and the relative weight f of the fast motion τ_0.

In a similar manner we have appended a fast motion τ_0 to the Cole–Cole distribution. The parameter ϵ determines the width of the Cole–Cole part of the distribution. τ_1/τ_0 specifies the separation between the peak of the Cole–Cole distribution and the fast motion, τ_0. The weight of the fast component is determined by f.

V. Results

Methylene T_1s. An exponential correlation function cannot describe the data for C4. Although this function does produce an extreme narrowing regime roughly in agreement with the data, the predicted T_1 minima are too low. The predicted value of nT_1/ω_C is 2.3×10^{-10} s^2 at the T_1 minima, while the experimental value is 4.0×10^{-10} s^2. The best fit of the C4 T_1 data to a single-exponential CF(t), indicated in Table II, has $\chi_R^2 = 5.9$. The calculated

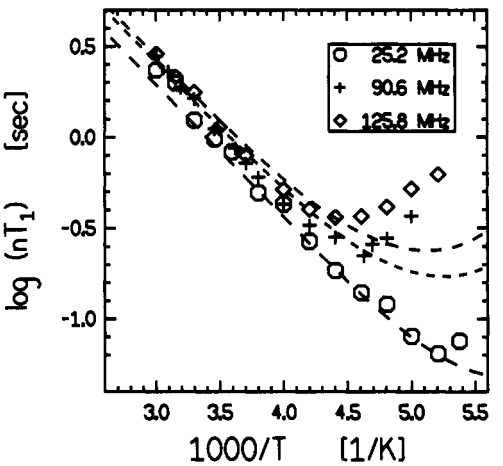

Figure 3. Best fit of the Cole–Cole distribution to spin–lattice relaxation data from the methylene carbon C4 of polyisoprene in toluene-d_8 solution. The points are experimental nT_1 values collected at three Larmor frequencies. The curves are calculated from the Cole–Cole model with $\epsilon = 0.79$, $E_a = 14.3$ kJ/mol, $A = 0.062$ ps/cP$^\alpha$, and $\chi_R^2 = 4.3$. Experimental error bars (±10%) are given by the size of the symbols. The Cole–Cole model and other unimodal distributions of motional time constants cannot fit the data.

barrier height is lower than the value extracted from the extreme narrowing regime.

None of the unimodal distributions can describe C4 T_1 data. It is possible for the Cole–Cole function to predict raised T_1 minima, in accordance with experiment. However, this requires broadening the distribution $F(\tau)$ so greatly that T_1 always depends strongly on ω_C. An extreme narrowing region cannot be reached. The best compromise, shown in Figure 3 and Table II, has $\chi_R^2 = 4.3$. The predicted T_1 minima are too low and occur at temperatures too cold. At high temperatures the model predicts a strong dependence on Larmor frequency. This is not seen in the data. Similar results were obtained with the Fuoss–Kirkwood and log χ^2 distributions. Best fits are included in Table II.

On the other hand, a biexponential CF(t) can fit the data quite well, if the two time constants are well separated. Figure 4 shows an example with $\tau_1/\tau_0 = 1000$. This fit has $\chi_R^2 = 1.08$. The values of f, A, and E_a all are stable within 1% as long as $\tau_1/\tau_0 \geq 500$.

The Hall–Helfand model cannot describe the data. Small values (≤5) of the ratio τ_2/τ_1 produce distributions $F(\tau)$ which closely resemble that of the single exponential. When large values of τ_2/τ_1 are used, the extreme narrowing regime is not reached until temperatures are too high. These fits also produce activation energies that are too

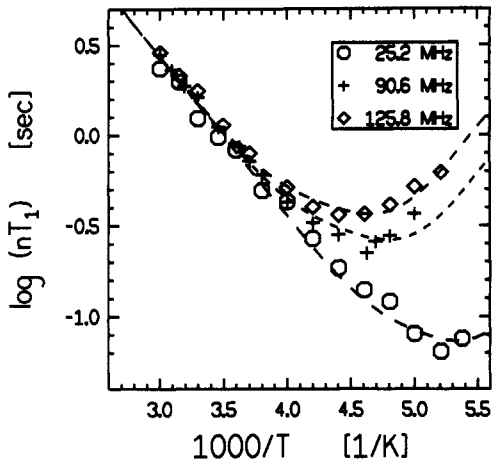

Figure 4. Best fit of the biexponential correlation function to nT_1 data from the methylene carbon C4 of polyisoprene in toluene-d_8 solution. The data points are the same as in Figures 1 and 3. The curves are calculated from the biexponential CF(t) with $\tau_1/\tau_0 = 1000$, $f = 0.495$, $E_a = 13.3$ kJ/mol, $A = 0.39$ ps/cP$^\alpha$, and $\chi_R^2 = 1.08$. Experimental error bars (±10%) are given by the size of the symbols.

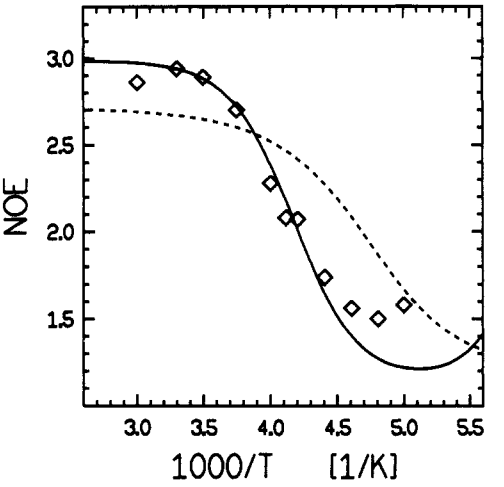

Figure 5. Temperature dependence of NOE ($\omega_C/2\pi = 125.8$ MHz) for the methylene carbon C4 of polyisoprene in toluene-d_8. The solid line is the prediction of the best fit biexponential CF(t) to T_1 data. The broken line is predicted by the best fit of the Cole–Cole model. All parameters are derived from the T_1 analysis only (Figures 3 and 4).

large ($E_a \geq 18$ kJ/mol if $\tau_2/\tau_1 \geq 100$). The best compromise is indicated in Table II.

The DLM CF(t) simplifies to the biexponential CF(t) when $\tau_1 \rightarrow \infty$. Interestingly, it is in this limit that the DLM function best describes the data. Restricting $\tau_1/\tau_0 = 1000$, the DLM predictions of the methylene T_1 data deteriorate rapidly as τ_2/τ_1 increases from 1 (see Table II). Holding $\tau_2/\tau_1 = 1$, the DLM predictions agree with the data if $\tau_1/\tau_0 \geq 500$. In this limit the values of f, A, E_a, and χ_R^2 are stable (with respect to changes in τ_1/τ_0) within 2%.

The overall best fit to the methylene T_1 data is produced by the modified Cole–Cole distribution, which allows rapid motion with time constant τ_0 and a Cole–Cole distribution of slower motions centered around τ_1. When $\epsilon = 1$ this distribution is identical with that of the biexponential CF(t). As ϵ is reduced to 0.95, slightly broadening the distribution of slower motions, χ_R^2 falls to a minimum of 0.99. This fit has $E_a = 14.5$ kJ/mol, slightly higher than, but within the specified uncertainty of, the value $E_a = 13 \pm 2$ kJ/mol extracted from our earlier study. Further decreasing ϵ leads to worse agreement with the data, particularly for $\epsilon < 0.9$.

Methylene NOEs. In some respects nuclear Overhauser enhancements provide a more stringent test of motional models than do T_1s.[9] At high temperatures, if T_1 reaches an extreme narrowing regime, the NOE should equal 3, its maximum value. As T_1 approaches a minimum, the NOE decreases. Broad distributions $F(\tau)$, which predict broad and high T_1 minima, also predict slow decreases in NOE as the temperature is lowered. Narrow distributions $F(\tau)$ predict relatively sharp T_1 minima and rapid decreases in NOE at temperatures near the T_1 minimum. Once the T_1 data have been fit, yielding a temperature dependence and shape of $F(\tau)$, no new parameters are required to predict NOE as a function of temperature. The NOE therefore provides an independent check of the shape of $F(\tau)$.

All of the conclusions from the T_1 analysis are supported by the NOEs. Figure 5 shows the experimental C4 NOEs at $\omega_C/2\pi = 125.8$ MHz. The solid curve shows the prediction of the biexponential CF(t), using parameters derived from the T_1 analysis. The agreement with the data is quantitative, except at the lowest temperatures where small deviations are observed. The dashed curve

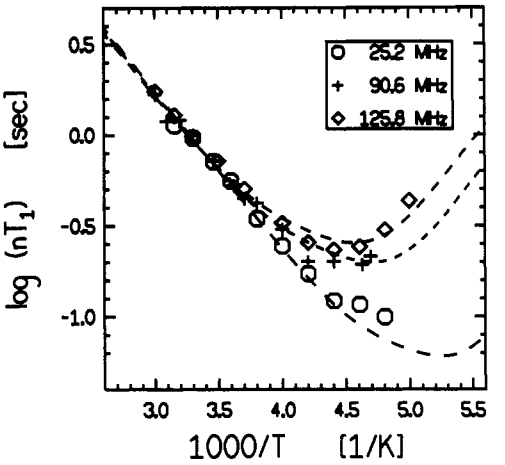

Figure 6. Best fit of the biexponential correlation function to nT_1 data from the methine carbon C3 of polyisoprene in toluene-d_8 solution. The curves are calculated from the biexponential CF(t) with $\tau_1/\tau_0 = 1000$, $f = 0.43$, $E_a = 13.2$ kJ/mol, $A = 0.53$ ps/cP$^\alpha$, and $\chi_R^2 = 1.22$. Experimental error bars (±10%) are given by the size of the symbols.

is the prediction of the Cole–Cole model. The Cole–Cole distribution does not predict NOE = 3 at the highest experimental temperatures, and the predicted NOE decreases too slowly with temperature. The C4 NOEs collected at 90 MHz show similar agreement with the biexponential CF(t) prediction and disagreement with the Cole–Cole model, but the data are considerably noisier.

Exactly those models that successfully describe T_1 data simultaneously describe NOE results. With parameters derived from the T_1 analysis, the biexponential, DLM, and modified Cole–Cole models quantitatively predict the NOEs. The single exponential, Hall–Helfand, Cole–Cole, Fuoss–Kirkwood, and log χ^2 models qualitatively disagree with the data.

Methine T_1s. The major characteristics of the C4 T_1 analysis are all reproduced in fitting the methine carbon spin–lattice relaxation times. Figure 6 shows the data as well as a fit using the biexponential CF(t). The values of f, A, E_a, and χ_R^2 are constant within 1% if $\tau_1/\tau_0 \geq 500$.[33]

In a manner similar to the C4 analysis, the biexponential, DLM, and modified Cole–Cole functions adequately reproduce the data. The single exponential, Hall–Hel-

Table III
C3 T_1 Fit Parameters

model	width[a]	τ_1/τ_0	f	E_a, kJ/mol	A, ps/cP$^\alpha$	χ_R^2
exponential				10.4	0.91	3.9
Cole–Cole	0.85			13.1	0.20	3.0
Fuoss–Kirkwood	0.84			12.5	0.27	3.2
log χ^2	39			13.3	0.17	2.6
biexponential		1000	0.43	13.2	0.53	1.22
Hall–Helfand	11			13.0	0.15	2.5
DLM	1	1000	0.41	13.6	0.78	1.30
modified Cole–Cole	0.95	1000	0.40	14.0	0.32	1.32

[a] Width corresponds to ϵ, β, p, or τ_2/τ_1.

fand, Cole–Cole, Fuoss–Kirkwood, and log χ^2 models cannot provide adequate fits. Best fit parameters are given in Table III.

VI. Discussion

The conclusions drawn in this paper are entirely consistent with our earlier work.[2] The most important new finding is that motion occurs on two well-separated time scales. None of the unimodal distribution functions can adequately describe T_1 or NOE data. Although the Hall–Helfand $F(\tau)$ has two peaks, it cannot reproduce the experimental T_1 values because no clean separation exists between them. On the other hand, the functions that invoke motion on two distinct time scales consistently provide excellent agreement with experiment.

The slower class of motions has τ in the vicinity of $1/\omega_C$. These dynamics are activated transitions, which we believe reflect conformational changes about backbone C–C single bonds. The other class of motions corresponds to $\tau \ll 1/\omega_C$. Our experiments are not sensitive to the temperature dependence of these dynamics, but we presume they are not activated. These fast motions are probably librations, reflecting wobbling motion of C–H bonds within potential energy wells.

Over the entire temperature range studied in toluene-d_8, the conformational motions have the temperature dependence of eq 11 with $E_a = 13 \pm 2$ kJ/mol and $\alpha = 0.41$. These values are consistent with the temperature and viscosity dependence of local dynamics at high temperatures in nine other solvents.[2] We believe that the extension to lower temperature in toluene-d_8 exemplifies what would be found in other solvents.

The superposition of T_1 data in Figure 1 demonstrates that the width of the distribution of time constants describing conformational dynamics does not change with temperature. The fact that a single τ (as in the biexponential CF(t)) is sufficient to describe conformational motions indicates that the distribution is narrow. The DLM and modified Cole–Cole models allow broader distributions of conformational time constants. However, these models can only describe the experimental data when the width of the distribution becomes very narrow; $\tau_2/\tau_1 \leq 1$ for the DLM function, or $\epsilon \approx 0.95$ for the modified Cole–Cole spectrum. This value of ϵ corresponds to a fwhm spread of a factor of 1.4 in τ.

Much less can be concluded about the fast librational motion. These motions are extremely rapid and account for roughly 50 and 40% of the CF(t) decays for C4 and C3, respectively (from the values of f). We have modeled librations as a δ function in $F(\tau)$ and assumed that they have the same temperature and viscosity dependence as conformational motions. However, this model is probably incorrect in detail. As pointed out in section III, T_1s (and NOEs) are insensitive to the shape of $F(\tau)$ for $\tau \ll 1/\omega_C$. This limit is appropriate for librational motions.

The conformational and librational motions are separated in time scale by a factor of 500 or more at low temperature. This restriction arises from the shape of the data (Figure 1 or 4) on the cold side of the T_1 minima, in particular the lowest temperature points. At 200 K the biexponential CF(t) suggests $\tau_{conf} \approx 2.2$ ns, and therefore $\tau_{lib} \leq 4$ ps. At higher temperatures the separation between conformational and librational motions may be less distinct. We believe τ_{lib} is too rapid to reflect thermally activated transitions. If, as is conceivable, τ_{lib} is essentially independent of temperature, τ_{conf}/τ_{lib} may be as small as 8 at 333 K. Fits of the biexponential CF(t) to the data improve slightly if τ_{lib} is held equal to 4 ps, independent of temperature.

The amplitude of librational motion can be estimated from the experimental data. The parameter f is determined almost entirely by the values of K and T_1 at the minima. Howarth[34] has proposed a restricted rotation model which assumes that the C–H bond can with equal probability adopt any orientation within a cone of half-angle Θ_m. Rapid motion within this cone quickly reduces the value of CF(t) to $(1 - f)$. Conformational dynamics are responsible for the remaining decay of CF(t). For our values of f Howarth's model predicts $\Theta_m \approx 35°$.

Dejean de la Batie and co-workers have proposed that τ_{lib} reflects motions within torsional potential energy wells, as opposed to activated transitions between wells.[31] We argue that this is plausible by showing that a reasonable potential energy surface for polyisoprene would allow rapid motions of roughly the observed amplitude. Other workers in our laboratory have estimated the torsional potential energy surface for polyisoprene.[6] Harmonic oscillations within these wells have oscillatory frequencies of approximately 1–8 THz. This provides a lower limit on τ_{lib} and demonstrates that librations on the picosecond time scale are plausible. Thermal energy enables C–H vectors to explore half-angles of 15–30° in the calculated, one-dimensional, torsional potential energy curve for polyisoprene. The cone of angles available for libration of a given C–H vector presumably reflects contributions from at least the two neighboring torsional angles. Hence a model of motion within a torsional potential is reasonably consistent with the experimental observations.

The above model implies that the time scale for librations should be only very weakly dependent on solvent viscosity. Recent Raman line shape experiments by MacPhail and co-workers demonstrate that this is the case for butane in solution[35] and for neat 1,2-difluoroethane.[36] From our previous work we estimate[37] that the reorientation time of toluene at 200 K is ≈ 50 ps, much longer than τ_{lib}. Since solvent molecules move only slightly on the librational time scale, librations cannot be strongly sensitive to the solvent viscosity.

Ryzhov and Byershtein have demonstrated that broad infrared absorption bands of several glassy polymers are caused by torsional vibrations of molecular groups similar

in size to the polymer repeat units.[38] Their explanation of these bands stresses the importance of intermolecular potentials in determining the characteristics of the observed librational motion. This may provide an alternative approach for understanding the librational motions observed in our experiments.

VII. Comparison to Previous Work

Dilute Polyisoprene Solutions. Experiments in our laboratories have investigated the local dynamics of polyisoprene solutions through time-resolved optical spectroscopy.[4,5,39] The motion of an anthracene chromophore covalently bonded into the chain backbone was monitored. Such experiments provide a direct measure of $CF(t)$, albeit for a different vector than sensed by NMR. The correlation functions for labeled polyisoprene generally are well described by the Hall–Helfand model with $\tau_2/\tau_1 \approx 4$, reflecting a rather narrow spectrum $F(\tau)$. The mean relaxation times $\langle\sigma\rangle_{optical}$ are longer and more strongly dependent on solvent viscosity than are τ_{conf}, as has been discussed previously.[2]

The optical experiments show no direct evidence for librational modes. It is possible, however, that fast librational motions are partially responsible for the fact that the observed fundamental anisotropy $r(0)$ is less than 0.4. Since the observed $r(0)$ is 0.32,[39] the librations sensed in the optical experiment must have a considerably smaller amplitude than those deduced from the NMR results; $\Theta_{m,optical} \leq 22°$. At least two factors presumably contribute to this difference between the experiments: (i) The optical experiments sense motion of a vector along the chain backbone. NMR probes a vector more or less perpendicular to the backbone. Librations of vectors along the backbone, if they exist, most likely span smaller angles than do librations of perpendicular vectors. In the context of Howarth's model, more restricted librations correspond to smaller values of f. Thus, librational components of $CF(t)$ would probably be weaker in the optical experiments. (ii) Librations near the anthracene label may be damped by its presence.

Bulk Polyisoprene. The spectrum of time constants describing conformational motions is broader for bulk polyisoprene rubber than for dilute solutions. Dejean de la Batie et al.[8] found that the DLM function describes polyisoprene (92% cis) motions if $\tau_2/\tau_1 \approx 40$ and $\tau_1/\tau_0 \geq 150$. The range of conformational time constants, specified by τ_2/τ_1, is considerably larger than that found for dilute solutions in this work, where $\tau_2/\tau_1 \leq 1$.

^{13}C NMR relaxation experiments on bulk polyisoprene suggest the importance of librations but are not definitive. Dejean de la Batie et al. assumed that $F(\tau)$ does not change shape with temperature and found that the DLM model (with the parameters above) can reproduce polyisoprene data. Libration angles were calculated to be about 35° for methylene groups, similar to our value for dilute solution. The agreement is less good for C3, where $\Theta_m \approx 20°$ in bulk and 35° in solution. This discrepancy may be real or may be an artifact of the analyses (different values of K were used and spin relaxation with nonbonded protons may be more important in the bulk polymer).

On the other hand, Denault and Prud'homme employed $\log \chi^2$, Cole–Cole, and Jones–Stockmayer distributions to analyze ^{13}C T_1 and NOE data from bulk polyisoprene with a microstructure similar to that used in the work reported here. Experiments were reported only for temperatures above the T_1 minima. Unlike the work of Dejean de la Batie et al. and our work, they allowed the width of $F(\tau)$ to change with temperature. This introduces a large degree of flexibility to the fitting procedure. With this assumption unimodal distributions do fit the data. It is not necessary to invoke two classes of motions occurring on well-separated time scales. The disparity between these two analyses demonstrates the utility of plotting T_1 data in the manner suggested by Guillermo and co-workers (Figure 1). In this way the temperature dependence of the shape of $F(\tau)$ can be directly examined. A further discussion of this discrepancy is found in ref 40.

Other Polymers. Other authors have invoked librations to help interpret NMR data. Dejean de la Batie et al. have measured ^{13}C T_1s of three polymers (poly(vinyl methyl ether),[31] polyisoprene,[8] and polybutadiene[8]) in dilute solutions with a single solvent at a single Larmor frequency ($CDCl_3$, 25 MHz). Dais et al. have examined ^{13}C T_1s and NOEs of poly(β-hydroxybutyrate) in tetrachloroethane solution at two Larmor frequencies.[41,42] The DLM model can fit temperature-dependent ^{13}C relaxation data for all of these polymers. The authors have thereby shown that librations can account for the data. However, it has not been shown that librations are necessary to account for the data. For example, the Hall–Helfand and Jones–Stockmayer models, which do not include librations, also can fit the poly(β-hydroxybutyrate) data.

A major motivation for studying dilute polymer solutions is that dilute-solution dynamics serve as a prototype for local dynamics in bulk. Librations may contribute to reorientation of various local vectors in many different bulk polymer systems. Consideration of librations as part of the local dynamics has been used to interpret ^{13}C NMR relaxation data from several polymer melts, including poly(vinyl methyl ether),[31] poly(propylene oxide),[32] linear and cross-linked poly(ethylene oxides),[32] *cis*-1,4-polybutadiene,[8] and *cis*-1,4-polyisoprene.[8] Solid-state ^2H NMR experiments have demonstrated that librations of C–H and N–H bonds play a major role in the local dynamics of both the crystalline and glassy phases of Nylon 66.[43,44] FTIR absorption spectra of many polymeric glasses also suggest the presence of librational motion.[38]

VIII. Summary

Two types of motion are important in the reorientation of backbone polyisoprene C–H bonds. A frequency–temperature superposition of ^{13}C NMR T_1 data allows this conclusion to be drawn unambiguously. At 200 K in toluene these two classes of motion are well resolved in time scale, although the distinction is probably less sharp at higher temperatures. The slower set of motions are thermally activated transitions between torsional potential energy minima and reflect conformational changes about backbone carbon–carbon single bonds. The faster motions are librations within potential energy wells. These motions can be thought of as restricted rotations about C–C bonds.

Nuclear magnetic resonance experiments are most sensitive to the slower, conformational motions. We have applied a frequency–temperature superposition to analyze these movements. The part of the correlation function, or equivalently the part of the spectrum of time constants, reflecting conformational motions does not change shape with temperature. The width of the distribution of conformational time constants is very narrow, so only a single time constant τ_{conf} is needed to characterize all of the possible conformational transition processes. The temperature and viscosity variation of τ_{conf} is given by eq 11 from 200 to 333 K in toluene. This temperature range includes both the extreme narrowing region and the T_1 minima. We believe that toluene exemplifies generic solvent behavior, so that eq 11 should remain valid through the T_1 minima in other solvents as well.

Librational motions occur in less than a few picoseconds and are much faster than the inverse of the Larmor frequency. Our experiments demonstrate that librations account for nearly half of the correlation function decay, but little else can be concluded with certainty. The magnitude and time scale for librations seem to be determined by the intramolecular potential energy surface, with little contribution from the solvent structure, viscosity, or temperature.

Acknowledgment. This research was supported by the National Science Foundation (Grant DMR-8822076). D.J.G. is grateful for fellowship support from IBM. NMR experiments were performed in the Instrument Center of the Department of Chemistry, University of Wisconsin. We thank the staff for assistance. We also thank Alan English and Mike Jablonsky for helpful discussions.

Appendix. Characteristic Equations Describing Motional Models

Equations for $J(\omega)$ that are not included here can be found in the references.

Single Exponential

$$\mathrm{CF}(t) = e^{-t/\tau_1} \tag{12}$$

$$J(\omega) = \frac{\tau_1}{1 + (\omega\tau_1)^2} \tag{13}$$

Cole–Cole[15,27]

$$F(s)\,ds = \frac{1}{2\pi}\frac{\sin(\epsilon\pi)}{\cosh(\epsilon s) + \cos(\epsilon\pi)}\,ds \tag{14}$$

$$s = \ln(\tau/\bar{\tau}) \tag{15}$$

Fuoss–Kirkwood[15,27]

$$F(s)\,ds = \frac{\beta}{\pi}\frac{\cos(\beta\pi/2)\cosh(\beta s)}{\cos^2(\beta\pi/2) + \sinh^2(\beta s)}\,ds \tag{16}$$

where s is defined in eq 15.

log χ^2 [15,29]

$$F(\sigma)\,d\sigma = \frac{p}{\Gamma(p)}(p\sigma)^{p-1}e^{-p\sigma}\,d\sigma \tag{17}$$

$$\sigma = \log_b[1 + (b-1)\tau/\bar{\tau}] \tag{18}$$

Biexponential

$$\mathrm{CF}(t) = (1-f)e^{-t/\tau_1} + fe^{-t/\tau_0} \tag{19}$$

with $\tau_1 > \tau_0$.

Hall–Helfand[31,30]

$$\mathrm{CF}(t) = e^{-t/\tau_1}e^{-t/\tau_2}I_0(t/\tau_1) \tag{20}$$

$$F(\tau)\,d\tau = \frac{d\tau}{\pi\tau^2\sqrt{-(\tau^{-1} - \tau_2^{-1})(\tau^{-1} - \tau_2^{-1} - 2\tau_2^{-1})}} \tag{21}$$

if $(\tau_2^{-1} + 2\tau_1^{-1})^{-1} \le \tau \le \tau_2$ and $F(\tau) = 0$ elsewhere.

DLM[31]

$$\mathrm{CF}(t) = (1-f)e^{-t/\tau_1}e^{-t/\tau_2}I_0(t/\tau_1) + fe^{-t/\tau_0} \tag{22}$$

Modified Cole–Cole

$$F(s)\,ds = \left[\left(\frac{1-f}{2\pi}\right)\frac{\sin(\epsilon\pi)}{\cosh(\epsilon s) + \cos(\epsilon\pi)} + f\delta(\tau - \tau_0)\right]ds \tag{23}$$

$$s = \ln(\tau/\tau_1) \tag{24}$$

References and Notes

(1) Morris, R. L.; Amelar, S.; Lodge, T. P. *J. Chem. Phys.* **1988**, *89*, 6523.
(2) Glowinkowski, S.; Gisser, D. J.; Ediger, M. D. *Macromolecules* **1990**, *23*, 3520.
(3) Hyde, P. D.; Waldow, D. A.; Ediger, M. D.; Kitano, T.; Ito, K. *Macromolecules* **1986**, *19*, 2533.
(4) Waldow, D. A.; Johnson, B. S.; Babiarz, C. L.; Ediger, M. D.; Kitano, T.; Ito, K. *Polym. Commun.* **1988**, *29*, 296.
(5) Waldow, D. A.; Johnson, B. S.; Hyde, P. D.; Ediger, M. D.; Kitano, T.; Ito, K. *Macromolecules* **1989**, *22*, 1345.
(6) Adolf, D. B.; Ediger, M. D. In *Computer Simulations of Polymers*; Roe, R. J., Ed.; Prentice-Hall: Englewood Cliffs, NJ, 1991; p 154.
(7) Howarth, O. W. *J. Chem. Soc., Faraday Trans. 2* **1980**, *76*, 1219.
(8) Dejean de la Batie, R.; Lauprêtre, F.; Monnerie, L. *Macromolecules* **1989**, *22*, 122.
(9) Denault, J.; Prud'homme, J. *Macromolecules* **1989**, *22*, 1307.
(10) The symbol τ_c and term "correlation time" often are used in the context of particular motional models. Different types of motion all contribute to the time correlation function; each is characterized by its own time constant. In the NMR literature these time constants are often termed correlation times. This terminology is inconsistent with the definition of τ_c in our earlier work. We now refer to the time integral of the correlation function as $\langle\sigma\rangle$ to avoid confusion.
(11) Kramers, H. A. *Physica* **1940**, *7*, 284.
(12) Helfand, E. *J. Chem. Phys.* **1971**, *54*, 4651.
(13) Viovy, J. L.; Monnerie, L.; Brochon, J. C. *Macromolecules* **1983**, *16*, 1845.
(14) Weber, T. A.; Helfand, E. *J. Phys. Chem.* **1983**, *87*, 2881.
(15) Heatley, F. *Prog. Nucl. Magn. Reson. Spectrosc.* **1979**, *13*, 47.
(16) Heatley, F. *Annu. Rep. NMR Spectrosc.* **1986**, *17*, 179.
(17) Abragam, A. *The Principles of Nuclear Magnetism*; Clarendon Press: Oxford, 1961; Chapter VIII.
(18) Farrar, T. C. *An Introduction to Pulse NMR Spectroscopy*; Farragut Press: Chicago, 1987.
(19) Cyvin, J. S. *Molecular Vibrations and Mean Square Amplitudes*; Elsevier: Amsterdam, 1968.
(20) Pople, J. A.; Gordan, M. *J. Am. Chem. Soc.* **1967**, *89*, 4253.
(21) Stark, R. E.; Vold, R. L.; Vold, R. R. *Chem. Phys.* **1977**, *20*, 337.
(22) Jablonsky, M. J. Ph.D. Thesis, University of Wisconsin, 1990.
(23) Bevington, P. R. *Data Reduction and Error Analysis for the Physical Sciences*; McGraw-Hill: New York, 1969; p 237.
(24) Guillermo, A.; Dupeyre, R.; Cohen-Addad, J. P. *Macromolecules* **1990**, *23*, 1291.
(25) It is possible to include this effect by plotting log $[(nT_1/\omega_0)(1 + \phi\omega_0^2)]$ on the vertical axis. Here, ϕ represents the ratio $\omega_0^2T_1^{dd}/T_1^{CSA}$. We implemented this with the approximation $\phi = (\sigma_\parallel - \sigma_\perp)^2/75nK$. This procedure improves the superposition for the C3 T_1 data.
(26) Cole, K. S.; Cole, R. H. *J. Chem. Phys.* **1941**, *9*, 341.
(27) Connor, T. M. *Trans. Faraday Soc.* **1964**, *60*, 1574.
(28) Fuoss, R. M.; Kirkwood, J. G. *J. Am. Chem. Soc.* **1941**, *63*, 385.
(29) Schaefer, J. *Macromolecules* **1973**, *6*, 882.
(30) Hall, C. K.; Helfand, E. *J. Chem. Phys.* **1982**, *77*, 3275.
(31) Dejean de la Batie, R.; Lauprêtre, F.; Monnerie, L. *Macromolcules* **1988**, *21*, 2045.
(32) Dejean de la Batie, R.; Lauprêtre, F.; Monnerie, L. *Macromolecules* **1988**, *21*, 2052.
(33) The quality of the fits can be improved by increasing the CSA contribution to T_1 by increasing $(\sigma_\parallel - \sigma_\perp)$.
(34) Howarth, O. W. *J. Chem. Soc., Faraday Trans. 2* **1979**, *75*, 863.
(35) Cates, D. A.; MacPhail, R. A. *J. Phys. Chem.* **1991**, *95*, 2209.
(36) MacPhail, R. A.; Monroe, F. C. *Chem. Phys.* **1991**, *152*, 93.
(37) This value is obtained from τ_R = 2.5 ps at 333 K (from ref 2) and applying the Stokes–Einstein–Debye equation.
(38) Ryzhov, V. A.; Byershtein, V. A. *Polym. Sci. USSR* (*Engl. Transl.*) **1989**, *31*, 489.
(39) Adolf, D. B.; Ediger, M. D.; Kitano, T.; Ito, K. *Macromolecules*, submitted.
(40) Denault, J.; Morèse-Séguéla, B.; Séguéla, R.; Prud'homme, J. *Macromolecules* **1990**, *23*, 4658.
(41) Dais, P.; Nedea, M. E.; Morin, F. G.; Marchessault, R. H. *Macromolecules* **1989**, *22*, 4208.
(42) Dais, P.; Nedea, M. E.; Morin, F. G.; Marchessault, R. H. *Macromolecules* **1990**, *23*, 3387.
(43) Hirschinger, J.; Miura, H.; Gardner, K. H.; English, A. D. *Macromolecules* **1990**, *23*, 2153.
(44) Miura, H.; Hirschinger, J.; English, A. D. *Macromolecules* **1990**, *23*, 2169.